

Available Online at [www.jourcc.com](http://www.jourcc.com)Journal homepage: [www.JOURCC.com](http://www.JOURCC.com)

CrossMark

# Journal of Composites and Compounds

## Predictive modeling of compressive strength and Young's modulus in MWCNT/45S5 bioglass scaffolds for bone tissue engineering

Maryam Irandoost <sup>a,\*</sup>, Vahid Nekouie <sup>b, c,\*</sup>

<sup>a</sup> Department of Materials and Metallurgical Engineering, Amirkabir University of Technology, Tehran, Iran

<sup>b</sup> School of Engineering and Build Environment, College of Business, Technology and Engineering, Sheffield, Sheffield Hallam University, Sheffield S1 1WB, UK

<sup>c</sup> Materials and Engineering Research Institute, College of Business, Technology and Engineering, Sheffield, Sheffield Hallam University, Sheffield S1 1WB, UK

### ABSTRACT

The clinical application of 45S5 bioglass® in load-bearing bone regeneration is limited by its inherently low mechanical strength. While the incorporation of multi-walled carbon nanotubes (MWCNTs) has shown promise in enhancing the mechanical properties of bioglass scaffolds, the resulting non-monotonic response, characterized by an initial increase followed by a decline at higher CNT loadings, poses a significant challenge for predictive modeling. In this study, we present a physics-informed, data-driven framework to accurately predict both the compressive strength and Young's modulus of freeze-cast MWCNT/45S5 bioglass composite scaffolds. Our model integrates the Gibson–Ashby theory for porous architectures with a Gaussian reinforcement function that captures the optimal CNT loading and the detrimental effects of agglomeration. Calibrated against experimental data from Touri et al. (2013), the model achieves excellent agreement, predicting peak compressive strength (5.02 MPa) and Young's modulus (305.8 MPa) at CNT contents of 0.311 wt.% and 0.319 wt.%, respectively. Furthermore, Monte Carlo simulations were employed to quantify the probabilistic reliability of achieving target mechanical thresholds (>4.5 MPa for strength, >250 MPa for modulus). These analyses reveal a robust processing window (0.25–0.40 wt.% CNT) where mechanical performance is highly reliable, providing critical guidance for scaffold design.

©2025 UGPH

Peer review under responsibility of UGPH.

### ARTICLE INFORMATION

#### Article History:

Received 05 September 2025

Received in revised form 10 December 2025

Accepted 15 December 2025

#### Keywords:

Predictive modeling

MWCNT-reinforced bioglass

Compressive strength

Young's modulus

Bone tissue engineering

### 1. Introduction

Creating three-dimensional (3D) scaffold structures that replicate the physical and biological attributes of natural bone as a means of regenerating, replacing or repairing bone due to injury/disease is the function of bone tissue engineering [1, 2]. An optimal scaffold has many necessary properties, including biocompatible, porous and interconnected for nutrient transport and cell infiltration, biodegradable, and strong enough to endure mechanical stresses while healing occurs [3]. The materials investigated to date for use as scaffolds in order to create a supportive framework for living bone regeneration include the 45S5 Bioglass® material, which exhibits excellent bioactive, osteoconductive, and bonding characteristics with living bone [4–6]. However, current limitations in terms of brittleness or fracture

toughness hinder its utility as a load-bearing material [7]. Researchers are combining high performance reinforcements within the bioglass matrix using composite strategies to overcome these barriers. Carbon Nanotubes (CNTs) have been identified as viable reinforcement options for ceramic and bioactive glass materials due to their exceptional tensile strength (~100 GPa), moduli of elasticity (~1 TPa) and aspect ratios [8–10]. If delivered to the material in good dispersion, CNTs typically enhance mechanical properties through one or a combination of the crack deflection, bridging and pull-out mechanisms [11, 12]. Comparing MWCNTs 45S5 bioglass type scaffolds with original ones manufactured via the techniques of freeze casting and spark plasma sintering, it has been determined that MWCNTs substantially enhance both compressive strength, and modulus of elasticity [13–15].

\* Corresponding authors: Maryam Irandoost & Vahid Nekouie, Emails: [maryamirandoost@yahoo.com](mailto:maryamirandoost@yahoo.com), [v.nekouie@shu.ac.uk](mailto:v.nekouie@shu.ac.uk)

<https://doi.org/10.61882/jcc.7.4.7> This is an open access article under the CC BY license (<https://creativecommons.org/licenses/by/4.0/>)

The relevance of CNT-reinforced bioglass systems remains well recognized in the current literature [16, 17]. Eivazzadeh-KeihanIt et al. [17] reaffirmed the MWCNT/45S5 Bioglass composite as a benchmark system in carbon-based nanocomposites for bone tissue engineering, explicitly highlighting its non-monotonic mechanical response and the critical role of CNT dispersion quality. Similarly, Sreena et al. note that despite significant advances in composite design, predictive modeling of CNT–bioglass interactions, particularly accounting for porosity, agglomeration, and interface effects, remains underexplored [16].

The latter works collectively underscore a persistent gap: while CNT reinforcement of bioglass is widely acknowledged as promising, physics-informed, quantitative frameworks capable of predicting the optimal CNT loading window under processing-induced uncertainties are still lacking [16, 17]. Our work directly addresses this gap by introducing a hybrid modeling approach that bridges micromechanical theory with data-driven reinforcement kinetics, offering a rational design tool for next-generation bioglass scaffolds.

According to a study done by Touri et al. [14] when MWCNTs were added to 45S5 bioglass scaffolds through freeze casting, the total compressive strength increased 119% from 2.08 MPa to 4.56 MPa and the elastic modulus increased by 139% from 111.5 MPa to 266.6 MPa. Further increasing the MWCNT content above this amount (e.g. 0.5 wt.%) diminished mechanical performance because of agglomeration, decreased relative density, and a weakened bond between MWCNTs and 45S5 scaffolds. This behavior exhibits a non-monotonic behavior where an increase in the amount of MWCNTs initially results in improvement in mechanical properties before deteriorating at higher levels of reinforcement. Predictive modeling is considerably impacted by this non-monotonic behavior.

Traditional micromechanical systems [18-21] based on the Halpin-Tsai equations generally assume homogeneous dispersion of materials, uniform and complete bonding at the interface, and a straightforward reinforcement relationship, which limits their ability to adequately capture the complexity and nonlinearity of the behavioral responses generally associated with multiwall CNT-reinforced bioglass scaffolds. Additionally, factors such as those induced by processing, such as porosity (~63%) in freeze-cast scaffolds, the arrangement of CNTs along the scaffold and the presence of agglomerates (clumps) of CNTs within the matrix further complicate modelling efforts to provide accurate predictions regarding mechanical performance [14, 15].

In this study, we present a predictive modeling framework for the compressive strength and Young's modulus of freeze-cast MWCNT/45S5 bioglass composite scaffolds based on experimental data from Touri et al. [14]. A robust model for describing the nonlinear dependence of CNT mechanical properties on concentration is developed through phenomenological fitting with mechanistic factors, such as CNT dispersion quality, relative density affects, and bridging mechanisms. Additionally, Monte Carlo simulation [22] was used to quantify the uncertainty and probability of CNT distribution and agglomeration, providing a more accurate picture of scaffold performance for use in bone tissue engineering.

## 2. Materials and methods

### 2.1. Theoretical modeling of compressive strength

The compressive strength of porous scaffolds is governed by a complex interplay between their architectural porosity and the intrinsic properties of the solid phase. For open-cell foam-like

structures fabricated via freeze-casting, the Gibson–Ashby model provides a foundational theoretical framework [23, 24]. This model relates the effective compressive strength of the porous scaffold,  $\sigma^*$ , to the strength of the fully dense solid material,  $\sigma_s$ , and the relative density of the scaffold,  $\rho_{rel}=\rho/\rho_s$ , as follows:

$$\sigma^* = C\sigma_s(\rho_{rel})^n \quad (1)$$

where  $n$  is a geometric exponent (typically  $n=1.5$  for open-cell foams) and  $C$  is a dimensionless constant that accounts for microstructural details such as strut geometry and defects.

In the current study, the experimentally measured compressive strength of the pure 45S5 bioglass scaffold ( $V_{CNT}=0$  wt.%) is  $\sigma_0=2.08$  MPa, with a measured porosity of ~63%, yielding a relative density of  $\rho_{rel}=0.37$ . The strength of a fully dense 45S5 bioglass,  $\sigma_s$ , was estimated as 300 MPa [14].

By calibrating the Gibson–Ashby model to this baseline data point, the constant  $C$  was determined as 0.1051. While this model accurately describes the base scaffold, it cannot capture the non-monotonic reinforcement behavior observed upon the addition of multi-walled carbon nanotubes (MWCNTs). As reported by Touri et al. [14], the compressive strength initially increases with CNT content, reaching a maximum of 4.56 MPa at 0.25 wt.%, before declining at higher loadings (e.g., 2.67 MPa at 0.5 wt.%) due to CNT agglomeration and reduced relative density. To model this effect, a phenomenological Gaussian function was superimposed on the Gibson–Ashby baseline. This function represents the efficiency of CNTs as a reinforcing phase, which is optimal at a specific concentration and diminishes with both under-dosing and over-dosing (agglomeration). The final combined model for the compressive strength as a function of CNT weight fraction ( $V$ ) is:

$$\sigma^*(V) = C\sigma_s(\rho_{rel})^n \times [1 + A \exp\left(-\frac{(V - V_{opt})^2}{2\omega^2}\right)] \quad (2)$$

Where  $A$  is the dimensionless amplitude, representing the maximum relative enhancement in strength due to CNTs.  $V_{opt}$  is the optimal CNT weight fraction at which the reinforcement effect is maximized.  $\omega$  is the characteristic width of the distribution, governing the sensitivity of the mechanical properties to variations in CNT content. The model parameters are fitted to the experimental data from Touri et al. [14] using a non-linear least-squares regression.

### 2.2. Theoretical modeling of Young's modulus

The elastic modulus of porous scaffolds is critically dependent on both the intrinsic stiffness of the solid phase and the macroscopic architecture induced by the fabrication process. For open-cell foam-like structures, such as those produced by freeze-casting, the Gibson–Ashby model serves as a widely accepted theoretical foundation for correlating the effective elastic modulus of the scaffold,  $E^*$ , with the modulus of the fully dense solid material,  $E_s$ , and the scaffold's relative density,  $\rho_{rel}=\rho/\rho_s$  [24]. For the elastic modulus, the Gibson–Ashby relationship is expressed as:

$$E^* = CE_s(\rho_{rel})^n \quad (3)$$

where  $n$  is a structural exponent. While a value of  $n=1.5$  is typical for the compressive strength of open-cell foams, a higher exponent of  $n=2.0$  is theoretically and experimentally justified for the Young's modulus, reflecting the more pronounced sensitivity of elastic stiffness to porosity.

In this work, the experimentally measured Young's modulus of the pure 45S5 bioglass scaffold ( $V_{CNT}=0$  wt.%) is  $E_0=112.02$  MPa, with a porosity of ~63%, yielding a relative density of  $\rho_{rel}=0.37$ . The elastic modulus of a fully dense 45S5 bioglass,  $E_s$ , was

assumed to be 1000 MPa. By calibrating the Gibson–Ashby model to the baseline experimental data, the pre-factor  $C$  was found to be 0.821, ensuring the model accurately predicts the base modulus of the pure scaffold [14].

Similar to the compressive strength, the Young's modulus of the CNT-reinforced scaffolds exhibits a non-monotonic trend: it increases with CNT content up to an optimum of 0.25 wt.% before declining at 0.5 wt.%. This behavior is attributed to the dual role of CNTs: acting as a high-modulus reinforcing phase when well-dispersed, but introducing defects and reducing the effective load-bearing cross-section when agglomerated [14].

To capture this complex behavior, we again adopt a phenomenological Gaussian function to represent the CNT reinforcement efficiency. The final combined model for the effective Young's modulus as a function of CNT weight fraction ( $V$ ) is formulated as:

$$E^*(V) = CE_s(\rho_{rel})^n \times [1 + A' \exp\left(-\frac{(V - V'_{opt})^2}{2\omega'^2}\right)] \quad (4)$$

The parameters retain their physical meaning as in the strength model:  $A$  is the maximum relative enhancement in modulus due to CNT reinforcement,  $V_{opt}$  is the optimal CNT loading,  $w$  governs the width of the effective reinforcement window. To obtain these unknown parameters, the model is fitted to the experimental Young's modulus data from Touri et al. [14].

### 3. Results and discussion

Bioglass scaffolds made from the freeze-casting method of MWCNT of 45S5 glass composite material were created using a method called the freeze-casting method. The 45S5 glass was created by using the sol-gel method to prepare the glass powder, which had a particle size of less than 1 micron when ground down into powder form. MWCNT were added to the bioglass slurry at concentrations of 0%, 0.1%, 0.25%, or 0.5% of the bioglass powder concentration (mass per cent). The bioglass slurry had 20% volume solids while it also contained 1% polyvinyl alcohol (PVA) binder and 2% carboxymethyl cellulose as dispersant materials in distilled water.

To create a homogenous mixture and to reduce agglomeration of the glass powder, it was ball milled for 24 hours and ultrasonicated for 2 hours before casting the final pieces [14]. The green bodies were then formed into cylindrical shapes by unidirectionally freezing them in a copper mould using a liquid nitrogen cold finger.

The green pieces were then freeze-dried for 72 hours at  $-60^{\circ}\text{C}$  and 1.3 KPa and then sintered in an argon atmosphere at  $900^{\circ}\text{C}$  for 3 hours (heating rate:  $10^{\circ}\text{C}/\text{min}$ ) [14]. The final bioglass scaffolds displayed a lamellar like microstructure showing 63% overall porosity and pore sizes that ranged between 20-100 microns and that were similar in appearance to the internal structure of cancellous bone.

The mechanical testing involved preparing cylindrical specimens measuring 12 mm in diameter and 20 mm in height. Using a Zwick/Roell HCT 400/25 dynamic testing machine set to a crosshead speed of 1 mm/min, compressive strength and Young's modulus were determined per ASTM F-2150.

Each composition of the sample was tested in five replicates; therefore, the reported values are presented as mean  $\pm$  standard deviation. The compressive strength of the MWCNT-reinforced 45S5 Bioglass scaffolds can successfully be modelled using a combined framework, which combines the Gibson–Ashby theory of porous materials and a phenomenological Gaussian function developed to describe the non-linear reinforcing effect of CNTs [14].

### 3.1. Compressive strength modeling

#### 3.1.1. Compressive strength of base scaffold

For the pure bioglass scaffold ( $V_{\text{CNT}}=0$  wt.%), the Gibson–Ashby model was calibrated to match the experimentally measured compressive strength of 2.08 MPa. Using a relative density  $\rho_{\text{rel}}=0.37$  (corresponding to the measured porosity of 63%) and an assumed strength of the fully dense material  $\sigma_s=300$  MPa, the structural constant  $C$  was determined as 0.03081. This calibration ensured that the predicted base strength,  $\sigma_0=2.08$ , was in exact agreement with the experimental value [14].

#### 3.1.2. Compressive strength of MWCNT/45S5 bioglass scaffolds

The combined model, which incorporates the CNT reinforcement term, was fitted to the four experimental data points using non-linear regression. The resulting optimized parameters are obtained as  $A=1.413$ ,  $V_{\text{opt}}=0.311$ ,  $w=0.105$ . The highest point of additive effect on compressive strength occurs when considering adding CNTs in a dosage greater than the initial estimate of 0.25 weight percent CNT. As can therefore also be interpreted: an increase in dosage may produce a stronger, higher performing scaffold when employing CNTs.

The prediction of maximum compressive strength due to contrast to experimental observations was made using Eq. 4. The predicted maximum compressive strength was determined to be 5.02 MPa or approximately 141% greater than the compressive strength of the base scaffold; however, this does correspond to the maximum experimental value of 4.56 MPa (at CNT loading of 0.25 wt.%).

Therefore, although the values of maximum compression strengths as given by experiment and prediction differ slightly (0.25 wt.% CNT vs 0.35 wt.% CNT), it can conclusively be stated that the prediction model is able to represent clearly the general trend in the relationship between compressive strength and the amount of CNT loaded to the scaffold; the prediction model correctly represents the relationship observed in the experiment through the correct matching of peak and lowest compressive strengths produced during the experiment as illustrated in Fig. 1.

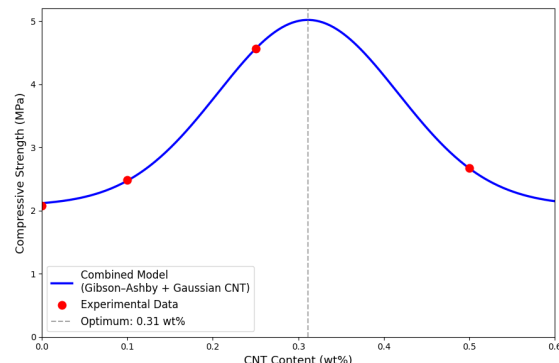


**Fig. 1.** Predicted compressive strength of MWCNT-reinforced 45S5 bioglass scaffolds as a function of CNT content (wt.%), based on the combined Gibson–Ashby and Gaussian reinforcement model. Experimental data points (red circles) are from Touri et al. [14].

The overall coefficient of variation is 0.27%. The predicted maximum CNT loading of 0.311 wt.% is invaluable for predicting future scaffold designs and provides evidence that the compressive strength of scaffolds tested at 0.25 wt.% could be increased slightly by making small changes in the amount of CNT loaded, assuming that proper dispersion and minimal agglomeration occur. The

philosophy of physics-informed, data-driven model gives a powerful prediction tool for determining the compressive strength of CNT reinforced bioglass scaffold materials with varying amounts of CNT, thus allowing for the rational design of biomaterials with specific mechanical properties for use in bone tissue engineering.

### 3.2. Young modulus modeling

The Young's modulus of the MWCNT-reinforced 45S5 bioglass scaffolds was successfully modeled using a combined framework that integrates the Gibson–Ashby theory for porous materials with a phenomenological Gaussian function to capture the non-linear reinforcement effect of CNTs.

#### 3.2.1. Young's modulus of base scaffold

For the pure bioglass scaffold ( $V_{\text{CNT}}=0$  wt.%), the Gibson–Ashby model was calibrated to match the experimentally measured Young's modulus of 112.02 MPa. Using a relative density  $\rho_{\text{rel}}=0.37$  (corresponding to the measured porosity of 63%) and an assumed modulus of the fully dense material  $E_0=1000$  MPa, the structural constant  $C$  was determined as 0.821. This calibration ensured that the predicted base modulus,  $E_0=112.02$  MPa, was in exact agreement with the experimental value [14].

#### 3.2.2. Young's modulus of MWCNT/45S5 bioglass scaffolds

The combined model, which incorporates the CNT reinforcement term, was fitted to the experimental data points using non-linear regression. The resulting optimized parameters are obtained as  $A=1.73$ ,  $V_{\text{opt}}=0.319$ ,  $w=0.10$ . According to these parameters, the maximum value of Young's modulus would occur at CNT loading above the 0.25 wt. % level which was noted in the experimental results, and within the upper end of the peak modulus range.

The peak Young's modulus predicted by the model is 305.84 MPa and it could provide a theoretical maximum increase in Young's modulus of approximately 172% compared to the base scaffold. The experimentally obtained value for Young's modulus at 0.25 wt.% was 265.82 MPa, which confirms that while there were some minor variations between the model and the experimental values, the model captures the overall trend. The model's predicted "rise-and-fall" behavior in Young's modulus corresponding to increasing CNT content corresponds to that seen in experiment (Fig. 2).

The model prediction recommends a CNT loading of 0.319 wt.% to optimise mechanical performance characteristics and to assist in defining optimal design criteria for the scaffold. It is important to note that a slight variation from the tested 0.25 wt.% will, in theory, improve mechanical performance, assuming that good dispersion quality and agglomeration control can be achieved.

This physics-informed, data-driven approach offers a robust tool for predicting the Young's modulus of CNT-reinforced bioglass scaffolds across a range of CNT loadings, facilitating the rational design of biomaterials with tailored elastic properties for bone tissue engineering applications.

It is important to note that the non-monotonic reinforcement behavior captured by our Gaussian function is not merely an empirical fit, but is physically grounded in the microstructural observations reported by Touri et al. [14].

Their SEM analyses clearly demonstrate that MWCNTs are homogeneously dispersed within the 45S5 Bioglass matrix at low

loadings (e.g., 0.25 wt.%), enabling effective load transfer and crack-bridging mechanisms.

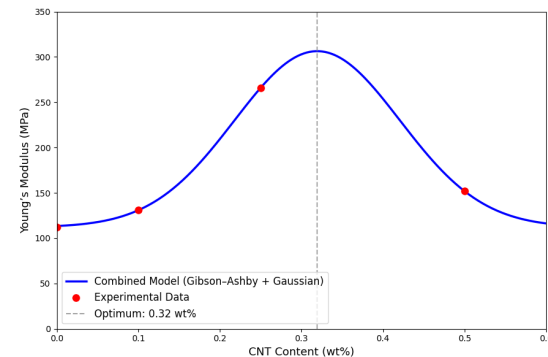


**Fig. 2.** Predicted Young's modulus of MWCNT-reinforced 45S5 bioglass scaffolds as a function of CNT content (wt.%), based on the combined Gibson–Ashby and Gaussian reinforcement model. Experimental data points (red circles) are from Touri et al. [14].

In contrast, at higher loadings (e.g., 0.5 wt.%), significant CNT agglomeration occurs, leading to stress concentration sites and weakened interfacial bonding, directly correlating with the observed decline in mechanical performance. Our model implicitly encodes this microstructure–property relationship through the peak position ( $V_{\text{opt}}$ ) and width ( $w$ ) of the Gaussian reinforcement term, thereby linking processing-induced dispersion quality to macroscopic mechanical response without requiring explicit image data.

## 4. Monte Carlo uncertainty quantification for MWCNT/45S5 bioglass scaffolds

A Monte Carlo simulation was conducted to account for the variability in all experimental parameters and processing parameters and also calculate the probability of obtaining a compressive strength of greater than the critical value of 4.5 MPa for the varying percentages of CNT loading. The analysis provides the evaluation of the reliability of the model in a probabilistic manner, which allows for determining the content of CNT most suitable for practical use. The Monte Carlo simulation was based on the previous calibrated model for the Gaussian reinforcement. In order to simulate real-life uncertainty in all parameters, each parameter was assumed to be normally distributed with a standard deviation of 10% of the nominal value. A total of 5000 Monte Carlo trials were completed for each of the levels of CNT from 0.0 to 5.0 wt%. The maximum probability of getting a compressive strength above 4.5 MPa was 53.3%, and this occurred at the CNT level of 0.256 wt%. At the experimentally reported optimum of 0.25 wt%, the probability of achieving a compressive strength above 4.5 MPa was 52.1%, which is close to the highest probability. The probability curve had a very sharp rise and fall around the optimum range of CNT, meaning that mechanical performance was indeed very sensitive to the CNT loading concentration. From the analysis performed under the assumption of a probabilistic approach, it has been found that whereas the deterministic analysis has identified an exact optimization for the amount of CNT in polymeric scaffolds (0.25 wt.%), due to the randomized nature of the real world, the fabrication will always introduce elements of uncertainty, and as such, there will not be one single guaranteed optimum point for this type of material, but instead, there will be a narrow range of probability (i.e. when the strength will be >50%) for the ranges from approximately 0.24 to approximately 0.27 wt%. By targeting a CNT loading of  $0.25 \pm 0.01$  wt.%, this design philosophy maximizes the likelihood

of producing polymer scaffolds with a compressive strength that is equal to or greater than 4.56 MPa (the value achieved in experiments). Higher or lower loadings significantly decrease (the probability of) producing polymer scaffolds with properties exceeding the experimental data at an optimized loading is primarily as a result of agglomeration or poor dispersion (discussed in detail in Section 3.2 of Touri et al. [14]). Consequently, as the optimal loading of CNTs is slightly above 0.25 wt.%, then even small modifications to either the methods of dispersing (and/or reducing the presence of agglomerates) CNTs during the fabrication process could result in potentially enhancing the mechanical performance without decreasing the reliability of the polymer scaffolds.

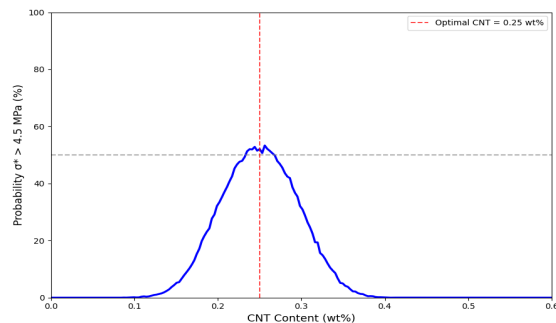


**Fig. 3.** Probability of achieving a compressive strength exceeding 4.5 MPa as a function of CNT content (wt.%), based on Monte Carlo simulation

The purpose of this analysis was to understand how probable it would be to get Young's Modulus values larger than 250 MPa for MWCNT reinforced 45S5 BioGlasses with different amounts of CNT loading through a Monte Carlo method based on experimental data gained from this study. This study was specifically designed not just to predict whether or not you would achieve success or fail but also to quantify the amount of confidence associated with achieving the desired characteristics of the scaffolds.

The simulation used the calibrations from the combination of Gibson-Ashby and Gaussian reinforcement models to create realistic test conditions through a variation of the experimental parameter set via simulating from a normal distribution. The sample was created through randomly selecting 20,000 points from a multi-dimensional normal distribution centered on the fitted parameters with the covariance matrix calculated from the curve-fitting process. The output for Young's modulus is illustrated in Fig. 4. The lowest concentration of CNT to achieve greater than 250 MPa on the deterministic model was around 0.23 wt.%, with a sharp transition between 0.23 wt.% and 0.24 wt.%, whereby the probability of achieving Young's modulus greater than 250 MPa increased to 100% and remained at this value until approximately 0.41 wt%. The 100% probability for achievement of Young's modulus greater than 250 MPa for this range of CNT concentrations indicates a broad range of reliable concentrations (0.235 wt% to 0.405 wt%) for scaffold fabrication. Based on the experimental optimum of 0.25 wt.%, the probability for achieving greater than 250 MPa is 100%, which demonstrates a high probability of reliability for this specific formulation. It should be noted that while the deterministic model shows that the optimal concentration is 0.319 wt.%, the inherent stochastic nature of CNT processing results in a range of probable concentrations (0.24 wt% to 0.40 wt%) to reliably achieve the desired Young's modulus.

The significance of this finding lies mainly in the manufacturing industry; it demonstrates how much variability can be tolerated in the CNT loading without causing an effect on performance. Practically, for scaffolds intended for load-bearing

bone tissue engineering applications (e.g., the natural spongy bone with a Young's modulus between 20-500 MPa, producing scaffolds with a Young's modulus that falls within the 0.25-0.40 wt.% range will represent the highest probability of success. The 0.25 wt.% represents the highest experimental peak for the Young's modulus, while higher CNT loading values produce predicted higher YMD, assuming that agglomeration occurs due to an improper dispersion technique that does not permit a sufficient separation of the CNTs. Furthermore, since the probability that CNTs provide a reinforcing effect within the 0.25 - 0.40 wt.% range is approximately 100% for that same range and beyond, we expect that during this window, they will continue to create bridging structures between the ceramic lamellae, as illustrated by Touri et al. in their SEM photomicrograph of CNT-reinforced bone scaffolds [14]. However, any increase in CNT content above 0.41 wt.% will cause the probability of producing scaffolds with a YMD of 0 to drop to zero as a consequence of the adverse effects of either agglomeration or reduced relative density, which are responsible for diminishing the interfacial bonding strength and lowering overall stiffness and strength [14].

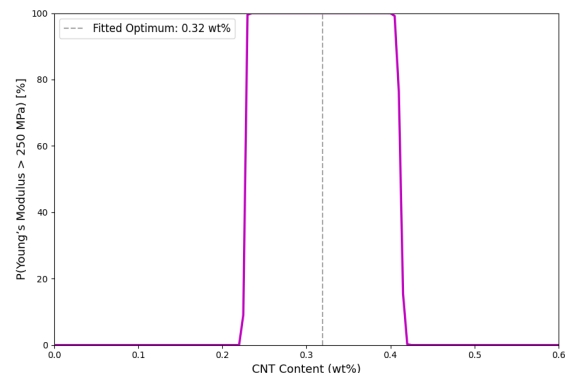


**Fig. 4.** Probability of achieving a Young's modulus exceeding 250 MPa as a function of CNT content (wt.%).

Ultimately, while Monte Carlo model validation is only a supporting function for the deterministic model, Monte Carlo simulation affords an evaluation of risk-aware algorithms to develop a robust and efficient scaffold with predictable performance levels and lower risk associated with physical properties such as mechanical performance. Therefore, controlling for the quantity of CNTs, as well as, controlling for the quality of the dispersion of CNTs will need to remain a focus of attention during the fabrication processes used to construct scaffolds intended for bone tissue engineering usage.

## 5. Conclusion

This research created a modeling framework that combines physics and data-driven methods to estimate the compressive strength and Young's modulus of freeze-cast MWCNT/45S5 Bioglass composite scaffolds using the experimental results published by Touri et al. [14]. By using the Gibson-Ashby theory for predicting the mechanical properties of porous materials and implementing a phenomenological Gaussian reinforcing model, the newly developed model accurately predicts the change in mechanical properties from the initial incrementation of CNTs to an optimal level of reinforcement, and subsequent decline in the reinforced materials' properties due to both agglomerates and a lower proportion of available relative density.

Using calibrated models, peak compressive strength and Young's modulus were predicted to be 5.02 MPa and 305.8 MPa respectively at CNT contents of 0.311 wt.% and 0.319 wt.%, in

close agreement with experimental peak values of 4.56 MPa and 265.8 MPa at a CNT content of 0.25 wt.%. The slight shift in the predicted optimum indicates that further improvement in the dispersion of CNTs, which can be accomplished with minor adjustments, may further enhance the mechanical properties of the composite material beyond the range tested by experimentation.

Monte Carlo uncertainty quantification has shown that all mechanical properties exhibited different reliability profiles. The probability of success for the compressive strength ( $> 4.5$  MPa) was found to be maximised in a narrow range of optimal performance (0.24 - 0.27 wt.% CNT content), with the probability of success being a maximum of 53.3%. Therefore, the compressive strength is sensitive to processing condition variability. Young's modulus ( $>250$  MPa) was found to give stable responses across a wide range of CNT loadings (0.235 - 0.405 wt.%) as evidenced by a 100% probability of success. Therefore, elastic stiffness is a very reliable design parameter and provides an indication of how to establish acceptable tolerance bands in mass production.

Using the findings of this study, we have come to the conclusion that CNTs are an excellent reinforcing mechanism for creating an in-depth model and optimization technique to allow for understanding how the composition (microstructure, composition (Mechanical)) of CNTs affect each other. As such, and providing a model framework to aid in the development of next-generation bone scaffolds with a risk awareness approach. Additionally, the fusion of deterministic prediction and probabilistic reliability provides us with a framework that supports rational designing of biomaterials with specified mechanical properties that fall within the physiological properties of cancellous bone to adequately use in load-bearing regenerative medicine clinics.

## Author contributions

**Maryam Irandoost:** Conceptualization, Writing – original draft, Writing – review & editing; **Vahid Nekouie:** Conceptualization, Writing – review & editing.

## Funding

No funding was received for this study.

## Conflict of interest

The authors declare no conflict of interest.

## Data availability

No data is available.

## REFERENCES

- [1] C. Liu, Z. Xia, J.T. Czernuszka, Design and development of three-dimensional scaffolds for tissue engineering, *Chemical Engineering Research and Design* 85(7) (2007) 1051-1064.
- [2] M. Selim, H.M. Mousa, M.U.A. Khan, G.T. Abdel-Jaber, N.M. Mubarak, A. Barhoum, A. Al-Anazi, A. Abdal-hay, Enhancing 3D scaffold performance for bone tissue engineering: A comprehensive review of modification and functionalization strategies, *Journal of Science: Advanced Materials and Devices* 9(4) (2024) 100806.
- [3] L. Suamte, A. Tirkey, J. Barman, P. Jayasekhar Babu, Various manufacturing methods and ideal properties of scaffolds for tissue engineering applications, *Smart Materials in Manufacturing* 1 (2023) 100011.
- [4] S. Smart, A. Cassidy, G. Lu, D. Martin, The biocompatibility of carbon nanotubes, *Carbon* 44(6) (2006) 1034-1047.
- [5] K. Sahithi, M. Swetha, K. Ramasamy, N. Srinivasan, N. Selvamurugan, Polymeric composites containing carbon nanotubes for bone tissue engineering, *International journal of biological macromolecules* 46(3) (2010) 281-283.
- [6] T. Ghasabpour, F. Sharifianjazi, L. Bazli, N. Tebidze, M. Sorkhabi, Bioactive glasses, ceramics, glass-ceramics and composites: State-of-the-art review and future challenges, *Journal of Composites and Compounds* (2025).
- [7] A.A. White, S.M. Best, I.A. Kinloch, Hydroxyapatite–carbon nanotube composites for biomedical applications: a review, *International Journal of Applied Ceramic Technology* 4(1) (2007) 1-13.
- [8] R. Sen, B. Zhao, D. Perea, M.E. Itkis, H. Hu, J. Love, E. Bekyarova, R.C. Haddon, Preparation of single-walled carbon nanotube reinforced polystyrene and polyurethane nanofibers and membranes by electrospinning, *Nano letters* 4(3) (2004) 459-464.
- [9] J.-E. Huang, X.-H. Li, J.-C. Xu, H.-L. Li, Well-dispersed single-walled carbon nanotube/polyaniline composite films, *Carbon* 41(14) (2003) 2731-2736.
- [10] T. Kuzumaki, O. Ujiie, H. Ichinose, K. Ito, Mechanical characteristics and preparation of carbon nanotube fiber-reinforced Ti composite, *Advanced Engineering Materials* 2(7) (2000) 416-418.
- [11] T. Laha, S. Kuchibhatla, S. Seal, W. Li, A. Agarwal, Interfacial phenomena in thermally sprayed multiwalled carbon nanotube reinforced aluminum nanocomposite, *Acta Materialia* 55(3) (2007) 1059-1066.
- [12] C. Deng, D. Wang, X. Zhang, Y. Ma, Damping characteristics of carbon nanotube reinforced aluminum composite, *Materials letters* 61(14-15) (2007) 3229-3231.
- [13] C. Balázsi, Z. Kónya, F. Wéber, L. Biró, P. Arató, Preparation and characterization of carbon nanotube reinforced silicon nitride composites, *Materials Science and Engineering: C* 23(6-8) (2003) 1133-1137.
- [14] R. Touri, F. Moztarzadeh, Z. Sadeghian, D. Bizari, M. Tahriri, M. Mozafari, The use of carbon nanotubes to reinforce 45S5 bioglass-based scaffolds for tissue engineering applications, *BioMed research international* 2013(1) (2013) 465086.
- [15] K.S. Munir, Y. Zheng, D. Zhang, J. Lin, Y. Li, C. Wen, Microstructure and mechanical properties of carbon nanotubes reinforced titanium matrix composites fabricated via spark plasma sintering, *Materials Science and Engineering: A* 688 (2017) 505-523.
- [16] R. Sreena, G. Raman, G. Manivasagam, A.J. Nathanael, Bioactive glass–polymer nanocomposites: a comprehensive review on unveiling their biomedical applications, *Journal of Materials Chemistry B* 12(44) (2024) 11278-11301.
- [17] R. Eivazzadeh-Keihan, Z. Sadat, F. Lalebeigi, N. Naderi, L. Panahi, F. Ganjali, S. Mahdian, Z. Saadatidizaji, M. Mahdavi, E. Chidar, Effects of mechanical properties of carbon-based nanocomposites on scaffolds for tissue engineering applications: a comprehensive review, *Nanoscale advances* 6(2) (2024) 337-366.
- [18] A. Montazeri, J. Javapour, A. Khavandi, A. Tcharkhtchi, A. Mohajeri, Mechanical properties of multi-walled carbon nanotube/epoxy composites, *Materials & Design* 31(9) (2010) 4202-4208.
- [19] Y. Zare, Development of Halpin-Tsai model for polymer nanocomposites assuming interphase properties and nanofiller size, *Polymer Testing* 51 (2016) 69-73.
- [20] M.K. Hassanzadeh-Aghdam, J. Jamali, A new form of a Halpin–Tsai micromechanical model for characterizing the mechanical properties of carbon nanotube-reinforced polymer nanocomposites, *Bulletin of Materials Science* 42(3) (2019) 117.
- [21] A.E. Hadi, M.H.M. Hamdan, J.P. Siregar, R. Junid, C. Tezara, A.P. Irawan, D.F. Fitriyana, T. Rihayat, Application of micromechanical modelling for the evaluation of elastic moduli of hybrid woven jute–ramie reinforced unsaturated polyester composites, *Polymers* 13(15) (2021) 2572.
- [22] M.J. Mahmoodi, M. Khamehchi, Random distribution of interphase characteristics on the overall electro-mechanical properties of CNT piezo nanocomposite: Micromechanical modeling and Monte Carlo simulation, *Probabilistic Engineering Mechanics* 75 (2024) 103577.
- [23] C. Chen, J. Ma, Y. Liu, G. Lian, X. Chen, X. Huang, Compressive behavior and property prediction of gradient cellular structures fabricated by selective laser melting, *Materials Today Communications* 35 (2023) 105853.
- [24] K. Ćwiek, J. Skibiński, Elastic properties of open cell metallic foams—modeling of pore size variation effect, *Materials* 15(19) (2022) 6818.